Dyes and Pigments 94 (2012) 266–270

Contents lists available at SciVerse ScienceDirect

Dyes and Pigments

journal homepage: www.elsevier.com/locate/dyepig

Enhancing photostability of cyanine dye by cucurbituril encapsulation

Hongyuan Zhang, Lele Liu, Chao Gao, Ruyi Sun, Qiaochun Wang*

Key Laboratory for Advanced Materials and Institute of Fine Chemicals, East China University of Science & Technology, No. 130 Meilong Road, Shanghai 200237, PR China

ARTICLE INFO

Article history:
Received 15 August 2011
Received in revised form
8 October 2011
Accepted 21 January 2012
Available online 28 January 2012

Keywords:
Pseudorotaxane
Cucurbituril
Cyanine dye
Photostability
Inclusion complex
Supramolecular chemistry

ABSTRACT

A linear cyanine dye (LDP) guest comprising two binding sites, one 4-[2-[4-(dimethylamino)phenyl] ethenyl]pyridinium group and one *p*-aminophenoxy ethylene group, was synthesized and proved could form inclusion complexes with cucurbit[7]uril (CB[7]) in aqueous solution. A partially encapsulated ([2]pseudorotaxane) state in which one CB[7] ring moved fast between the two binding sites was originally detected and was then transferred into a full encapsulated ([3]pseudorotaxane) state where two CB[7] macrocycles resided on both binding sites with the continuously adding of CB[7] to LDP. The two binding constants K_1 and K_2 were determined as $(6.29 \pm 0.88) \times 10^4\ M^{-1}$ and $(1.58 \pm 0.17) \times 10^4\ M^{-1}$, respectively. Compared with the free LDP, the photostability of the [3]pseudorotaxane is found been distinctively promoted, while that of the [2]pseudorotaxane state is hardly improved.

1. Introduction

The cyanine dyes are undoubtedly one of the most important classes of dyes for their extensive applications, for example, in the area of imaging sensitizer, DNA indicator, ion probe, as well as in data storage and dye-sensitized solar cell [1–7]. It is obvious that photobleaching of cyanine dyes is an undesirable characteristic in most cases. Efforts have been made to improve the stability in regard to the photochemical decomposition by structural modification or adding additives [8–10]. Yet, these methods are somewhat complex or less efficient. Anderson group has also reported a strategy to enhance the photostability of dyes by threading them into the cavity of cyclodextrin [11], but this effective method should be faced with challenging rotaxane construction. Cucurbiturils (CBs) are pumpkin-shaped macrocylic host molecules synthesized from the acid-catalyzed cyclization of glycoluril and formaldehyde. Like cyclodextrins, they are commercially available with good stability, and can form inclusion complexes with a variety of organic guests. Moreover, CBs have higher affinity and better selectivity than cyclodextrins especially for those guests with positive charge, thus could boost stable inclusion complex formation [12]. To the best of our knowledge, reports on slowing down the photobleaching of a dye with cucurbituril are extremely rare [13]. Herein we describe a facile method to reduce the photobleaching of a cyanine dye by simply mixing it with Cucurbit[7]uril (CB[7]) in aqueous solution to form a [3]pseudorotaxane.

2. Experimental

2.1. Chemicals and instruments

Cucurbit[7]uril was synthesized according to reported method [14]. Other reagents were commercially available and used without further purification.

^{1}H NMR spectra were recorded on a Brüker AM 400 spectrometer with tetramethyl silane (TMS) as internal reference. ESI-MS spectra were conducted on Waters LCT Premier XE mass spectroscopy. Absorption spectra and Fluorescence spectra were measured on a Varian Cary100 UV–Vis spectrophotometer and a Varian Cary Eclipse Fluorescence spectrophotometer, respectively. The photobleaching experiments were carried out by using a 500 W xenon lamp emitting visible light with an intensity of 14,000 wcm^{-2}. The photographs were taken by Pentax k–r digital single lens reflex camera.

2.2. Synthesis

2.2.1. Preparation of 1-[2-(4-Nitrophenoxy)ethyl]-4-methyl pyridinium bromide(**1**)

A mixture of 22.0 g (89.8 mmol) 1-(2-bromoethoxy)-4-nitrobenzene [15] and 12.0 g (129 mmol) 4-methylpyridine in

* Corresponding author. Tel. /fax: +86 2164252758.
E-mail address: qcwang@ecust.edu.cn (Q. Wang).

0143-7208/$ – see front matter © 2012 Elsevier Ltd. All rights reserved.
doi:10.1016/j.dyepig.2012.01.022

50 ml DMF was stirred at 100 °C for 10 h, then 60 ml ethyl acetate was added and the resulting mixture was stirred and cooled to room temperature, the precipitate was collected by filtration, washed with 50 ml ethyl acetate and dried to give 21.5 g (71%) **2** as a pale yellow solid. m.p. 240–242 °C; ^{1}H NMR (400 MHz, DMSO-d_6): $\delta = 8.84$(d, 2H, $J = 6.4$ Hz); 8.15(d, 2H, $J = 9.3$ Hz); 7.33(d, 2H, $J = 6.4$ Hz); 8.25(d, 2H, $J = 9.3$ Hz); 4.78(t, 2H, $J_1 = 4.6$ Hz, $J_2 = 4.8$ Hz); 4.59(t, 2H, $J_1 = 4.8$ Hz, $J_2 = 4.6$ Hz); 2.76(s, 3H)。

*2.2.2. Preparation of 4-[2-[4-(dimethylamino)phenyl]ethenyl]-1-[2-(4-nitrophenoxy)ethyl] pyridinium bromide (**2**)*

A mixture of 11.3 g (33.4 mmol) **1**, 6.0 g (40.3 mmol) 4-(dimethylamino)benzaldehyde and 90 ml ethanol was heated to 60 °C with stirring, then 1.0 ml piperidine was added and the solution was stirred under reflux for 6 h. After cooled to room temperature, the precipitate was collected by filtration, and recrystallized from ethanol to give 10.2 g (65%) **3** as a red solid. m.p. 269–271 °C; ^{1}H NMR(400 MHz, DMSO-d_6): $\delta = 8.82$(d, 2H, $J = 6.7$ Hz); 8.23(d, 2H, $J = 9.2$ Hz); 8.08(d, 2H, $J = 6.9$ Hz); 7.94(d, 1H, $J = 16.0$ Hz); 7.60 (d, 2H, $J = 8.9$ Hz); 7.19(d, 1H, $J = 16.0$ Hz); 7.16(d, 2H, $J = 9.3$ Hz); 6.79(d, 2H, $J = 9.0$ Hz); 4.89(t, 2H, $J = 4.6$ Hz); 4.65(t, 2H, $J = 4.6$ Hz); 3.04(s, 6H).

2.2.3. Preparation of 4-[2-[4-(dimethylamino)phenyl]ethenyl]-1-[2-(4-aminophenoxy)ethyl] pyridinium bromide (LDP)

To a solution of 10.0 g (21.3 mmol) **2** in 80 ml hot ethanol, was added 8.0 g (143 mmol) iron powder, 30 ml water and 1.0 ml 45% HBr with stirring. The resulting mixture was heated under refluxed for 4 h and filtered hot, the filtrate was concentrated by rotary evaporation and the resulting solid was recrystallized from ethanol twice to give 4.6 g (51%) LDP as a red powder. m.p. 251–253 °C; ^{1}H NMR (400 MHz, DMSO-d_6): $\delta = 8.78$(d, 2H, $J = 6.9$ Hz); 8.07(d, 2H, $J = 6.9$ Hz); 7.94(d, 1H, $J = 16.1$ Hz); 7.60(d, 2H, $J = 8.9$ Hz); 7.19 (d, 1H, $J = 16.1$ Hz); 6.79(d, 2H, $J = 9.0$ Hz); 6.63(d, 2H, $J = 8.8$ Hz); 6.49(d, 2H, $J = 8.7$ Hz); 4.77(t, 2H, $J = 4.7$ Hz); 4.31(t, 2H, $J = 4.7$ Hz); 3.03(s, 6H); MS (*m/z*): [M-Br]$^+$ calcd. for $[C_{23}H_{26}N_3O]^+$ 360.21; found: 360.2.

3. Results and discussion

3.1. The formation of inclusion complex

A dimethylamino phenyl moiety (DMA) and a *p*-aminophenoxy ethylene group (OA) were arranged at the two ends of LDP, as shown in Scheme 1. They were both proved as binding sites for CB[7] in our previous study [16], and as a result, a [3]pseudorotaxane might finally be obtained when one LDP molecule binds two CB[7] rings. To confirm the binding ratio, measurements of the fluorescence of a series of LDP solutions with different CB[7] molar fraction were carried out with a total concentration remaining constant. The resulting job plot curve is shown in Fig. 1. The maximum value of the vertical axle corresponds to 0.33 at horizontal axle, and the stoichiometry of LDP and CB[7] is verified to be 1:2.

Although a final [3]pseudorotaxane (abbreviated as LDP·CB_2) would form, LDP may also display as other different architectures when binding to CB[7] at low molar ratio. These are the [2]pseudorotaxanes (abbreviated as LDP·CB) in which one CB[7] macrocycle encircles either of the two binding sites. To investigate the inclusion behaviors of LDP and CB[7], the ^{1}H NMR spectra of LDP aqueous solution titrating with CB[7] were monitored. The ^{1}H NMR technique is a very efficient method to identify the binding site of CBs-based complex. It is a common rule that the protons inside the hydrophobic cucurbituril cavity undergo shielding effect while the outside ones conduct deshielding effects, and those near the carbonyl rim are hardly affected [17,18]. To prevent the protonization of the OA group, the ^{1}H NMR experiments were recorded at a weak base environment (pD = 9.6, and the pK_a of OA

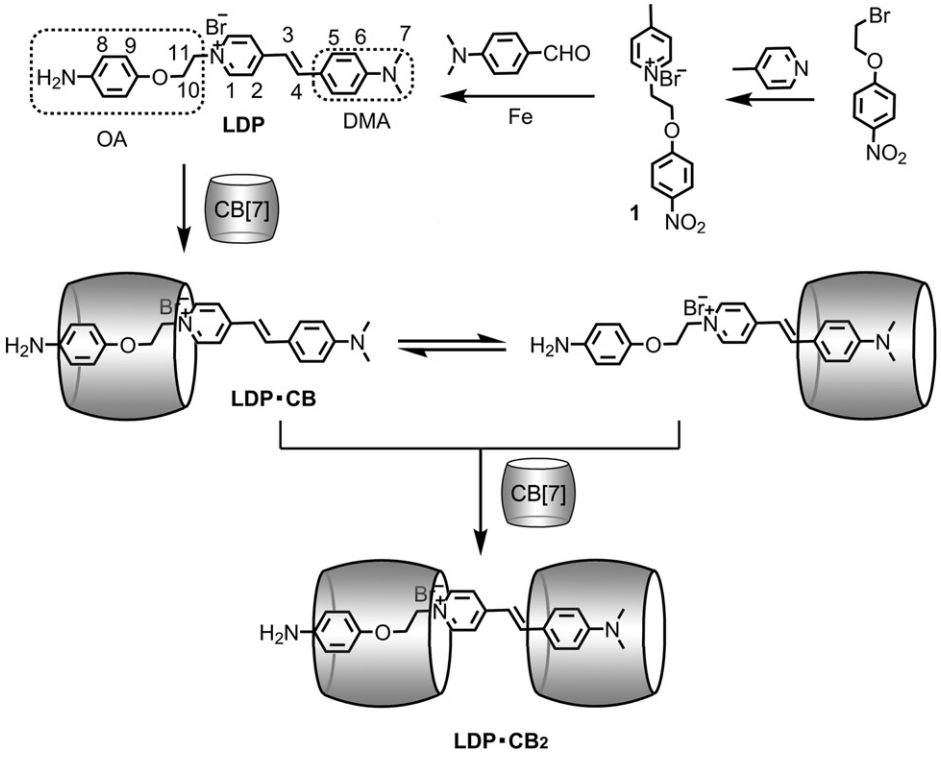

Scheme 1. Synthetic route of cyanine dyes LDP and its complexation behavior with CB[7].

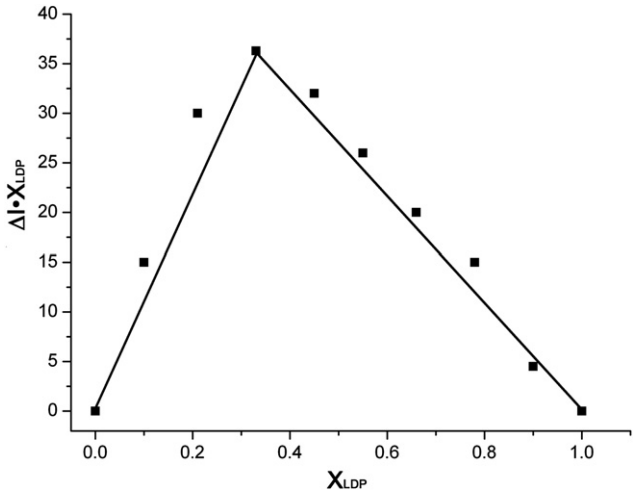

Fig. 1. Job plot for the complexation of LDP and CB[7] (the total concentration of CB[7] and LDP is 50 mM at pH = 9.6).

is 7.31 after encapsulated by CB[7] [16]), as illustrated in Fig. 2. Compared with LDP alone (Fig. 2a), most protons of LDP with the increasing addition of CB[7] (Fig. 2c) were found shift distinctly. On one hand, the pyridine proton H_2 experiences a downfield-shift ($\Delta\delta_{H2}$ increases from +0.11 ppm in 0.5 equiv to +0.25 ppm in 4.0 equiv) and the OA protons H_8, H_9, H_{10}, H_{11} upfield-shift ($\Delta\delta_{H8}$ is −0.19 ppm in 0.5 equiv and −0.40 in 4.0 equiv; $\Delta\delta_{H9}$ is −0.20 ppm in 0.5 equiv and −0.48 ppm in 4.0 equiv; $\Delta\delta_{H10}$ is −0.21 ppm in 0.5 equiv and −0.47 ppm in 4.0 equiv; $\Delta\delta_{H11}$ is −0.22 in 0.5 equiv and −0.48 ppm in 4.0 equiv). These facts mean that pyridinium group undergoes deshielding effect and OA site conducts shielding effect, and a CB[7] ring residing over the OA moiety can thus be deduced. On the other hand, shielding effects on the DMA group ($\Delta\delta_{H5}$ is −0.03 ppm in 0.5 equiv and −0.31 ppm in 4.0 equiv; δ_{H6} is −0.03 ppm in 0.5 equiv and −0.21 ppm in 4.0 equiv; $\Delta\delta_{H7}$ is −0.03 ppm in 0.5 equiv and −0.49 ppm in 4.0 equiv) and the deshielding effects on the vinyl unit ($\Delta\delta_{H3}$ is +0.03 in 0.5 equiv and +0.06 ppm in 4.0 equiv; and $\Delta\delta_{H4}$ is +0.05 ppm in 0.5 equiv and +0.09 ppm in 4.0 equiv) can also be found. These phenomena show that there is also a CB[7] ring staying at the DMA moiety. The above two deductions seem inconsistent when the molar ratio of CB[7]/LDP is lower than 2.0 equiv. However, when taking into account the fact that there are only increasing movements but not splitting of the proton signals observed with the continuously increasing of the molar ratio of CB[7]/LDP until the full [3]pseudorotaxane (for example CB[7]/LDP = 4.0 in Fig. 2d) is realized, we can come to the conclusion that the CB[7] ring undergoes fast exchanging between the two binding sites till they are both encapsulated. Moreover, in view of the obvious deshielding effect of the pyridinium vinyl moiety, the exchanging route should be OA—solvent—DMA (Scheme 1), but not OA—pyridinium—DMA (in this manner, the pyridinium group should be in shielding region).

At the condition that pH<7.31, the OA group would be protonized and according to the common rule, CB[7] should stay at the dicationic side. But unfortunately, though repeated efforts had been made, we did not get the clear NMR signals (the best NMR spectrum among these is shown in Fig. 2f) to confirm the exact architecture of the complex. Taking into account that the protonated LDP molecule can be regarded as another cyanine dye, we did not carry out further investigation.

3.2. Binding constants

The above investigations show that, with the increasing addition of CB[7] to the LDP aqueous solution, LDP·CB comes into being where CB[7] moves fast between the two binding sites and then is transferred into the 1:2 complex LDP·CB_2. The association equilibrium can be written as the following equation (Eq. (1)):

$$\begin{aligned} &\mathrm{LDP} + \mathrm{CB[7]} \overset{K_1}{\rightleftharpoons} \mathrm{LDP{\cdot}CB} \\ &\mathrm{LDP{\cdot}CB} + \mathrm{CB[7]} \overset{K_2}{\rightleftharpoons} \mathrm{LDP{\cdot}CB_2} \end{aligned} \tag{1}$$

The gradual addition of CB[7] to LDP up to about 50 equiv leads to a remarkable increase in the fluorescence intensity by 14 folds, as can be seen from Fig. 3. This exciting observation should result from the increasing rigidity [19] and the reduced environment polarity [20] when LDP enters into the cavity of CB[7]. The binding constants K_1 and K_2 are calculated by analyzing the gradual changes in the intensity of the fluorescence with the increasing concentration of the host. The detected fluorescent intensity I_f at any stage

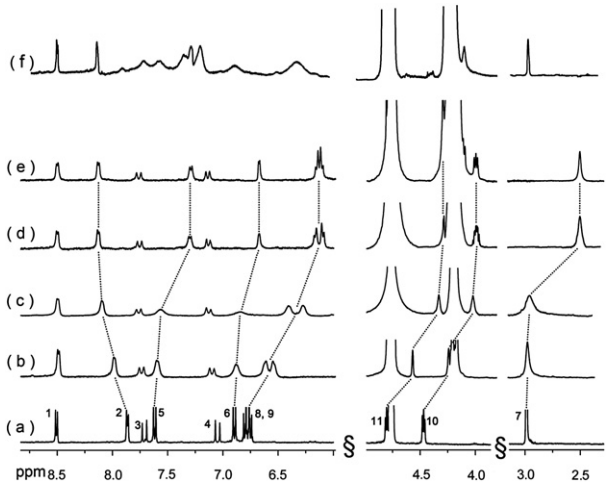

Fig. 2. ^{1}H NMR spectra (400 MHz, D_2O) of LDP (3 mM) at pD = 9.6 in different environment: (a), LDP alone, (b) LDP and 0.5 equiv CB[7], (c)LDP and 1.1 equiv CB[7], (d) LDP and 4 equiv CB[7], (e) LDP and 5 equiv CB[7]. (f) At pD = 6.5 with 1.1 equiv CB[7].

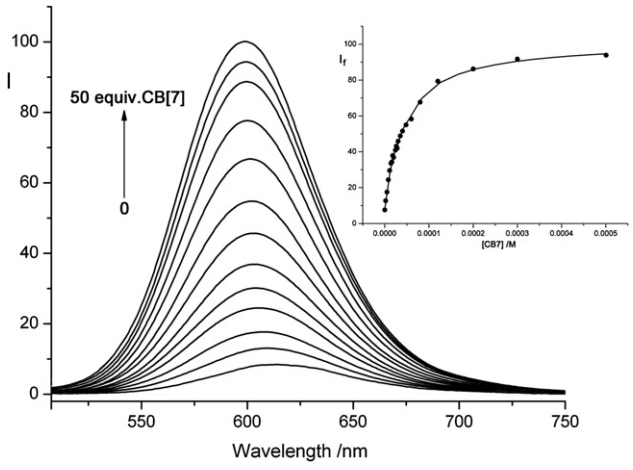

Fig. 3. The emission spectrum of LDP (1×10^{-5} M in H_2O) in the presence of increasing concentration of CB[7] (0–50 equiv) at pH = 9.6. Inset: the experimental data shows the best fit to the 1:2 binding model at 599 nm.

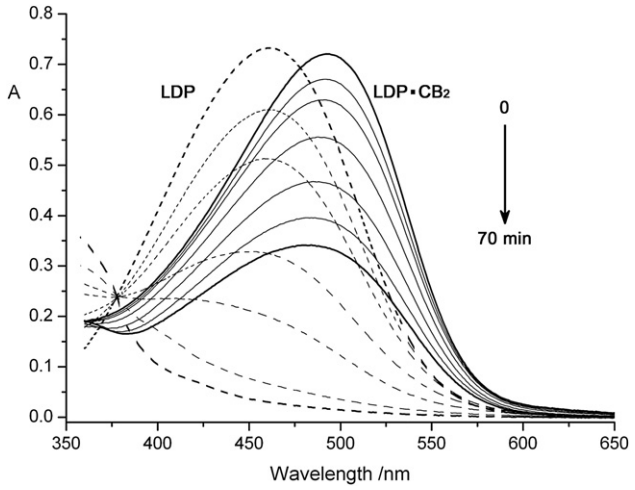

Fig. 4. UV–Vis absorption spectral changes of LDP (dash line) and the LDP·CB_2 (solid line) complex (both LDP concentrations are 25 μM, and the latter 50 equiv of CB[7] added) in H_2O at pH = 9.6 upon irradiation (the irradiation intensity is 14,000 wcm^{-2}).

is contributed by LDP, LDP·CB and LDP·CB_2 according to the concentrations of their presence in the solution. So the calculation equation can be written as [21,22]:

$$I_f = \frac{I_f^0 + I_{LDP\cdot CB}K_1[CB]_0 + I_{LDP\cdot(CB)2}K_1K_2[CB]_0^2}{1 + K_1[CB]_0 + K_1K_2[CB]_0^2} \quad (2)$$

where K_1 and K_2 are the binding constants for the formation of the respective pseudorotaxanes LDP·CB and LDP·CB_2; I_f is the detected fluorescent intensity at any stage; I_f^0 is the fluorescent intensity of LDP in the absence of CB[7]; $I_{LDP\cdot CB}$ is the fluorescent intensity of the 1:1 inclusion complex; and $I_{LDP\cdot(CB)2}$ is the fluorescent intensity of the [3]pseudorotaxane. $[CB]_0$ is the total concentrations of the CB [7] used. The K_1 and K_2 were then estimated to be $(6.29 \pm 0.88) \times 10^4\ M^{-1}$ and $(1.58 \pm 0.17) \times 10^4\ M^{-1}$ after applying Eq. (2) to fit the fluorescent intensities at 599 nm at different concentration of CB [7], as shown in Fig. 3 inset.

3.3. Photostability

The absorption of LDP aqueous solution undergoes an intense bathochromic shift when the chromophore is encapsulated into the cavity of the CB[7], as illustrated in Fig. 4. The maximum absorption peak of LDP is found at 461 nm, and the color of the solution is yellow. The [3]pseudorotaxane aqueous solution shows a maximum absorption peak at 493 nm, which is a 32 nm bathochromic shift compared with the free LDP, and represents an obvious color change to orange red. The large red-shift is the result of the enhancement of intramolecular charge-transfer caused by the deshielding effect to the pyridinium unit and the shielding effect to the DMA moiety when the two binding sites are encapsulated by CB[7].

It is generally considered that CB[7] can prevent the dye from photo-oxidation and ozonolysis when a chromophore is encapsulated inside the CB[7] ring [23]. So it is expected that the photostability of LDP could be improved by adding CB[7]. The photostability investigation of LDP (25 μM) and its [3]pseudorotaxane LDP·CB_2 (25 μM LDP + 50 equiv of CB[7]) were then carried out. The two solutions were put into two quartz cuvettes respectively, and then exposed to the xenon lamp irradiation. Their fading processes were photographed, as shown in Fig. 5. The aqueous solution of LDP was thoroughly bleached after 70 min, whereas LDP·CB_2 still remained an evident color. Their relative absorption spectra are shown in Fig. 4. It shows that the absorption of the free LDP aqueous solution displays a sharp decrease with the continuous irradiation, while the LDP·CB_2 solution under the same situation is affected rather limitedly. The photobleaching rate constants were then calculated [24,25] according to the fading data, as can be seen in Fig. 6. The light-fading processes fit to the first-order kinetic decay curves, which are in accordance with the mechanism of the photobleaching of cyanine dyes [26,27], and the constants are determined as $k_L = 0.042\ min^{-1}$ and $k_{LC2} = 0.012\ min^{-1}$ (k_L and k_{LC2} are the photobleaching rate of LDP and LDP·CB_2 respectively). The promotion of the photostability through encapsulation is accordingly proved.

It is noteworthy that the 1:1 complex LDP·CB exhibits little photostability improvement relative to LDP alone. The light-fading

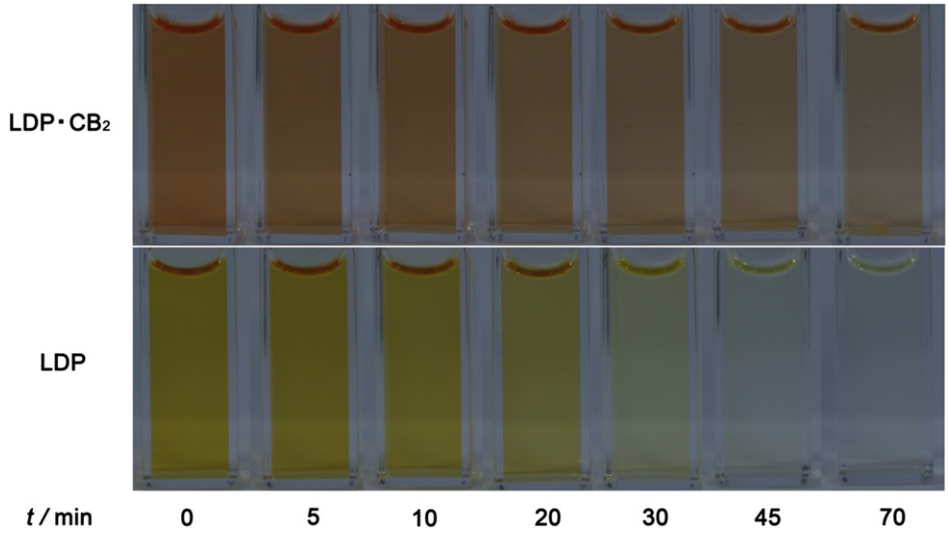

Fig. 5. The fading process of LDP (25 μM) and LDP·CB_2 (25 μM LDP + 1.25 mM CB[7]) at pH = 9.6 were recorded by camera with increasing irradiation time. The intensity of irradiation was constant with 14,000 wcm^{-2}. All the photos were shot at the same environment and parameters: Shutter speed: 1/20s; focal length: 35 mm; aperture: F/5; ISO: 200; exposure compensation: 0 EV.

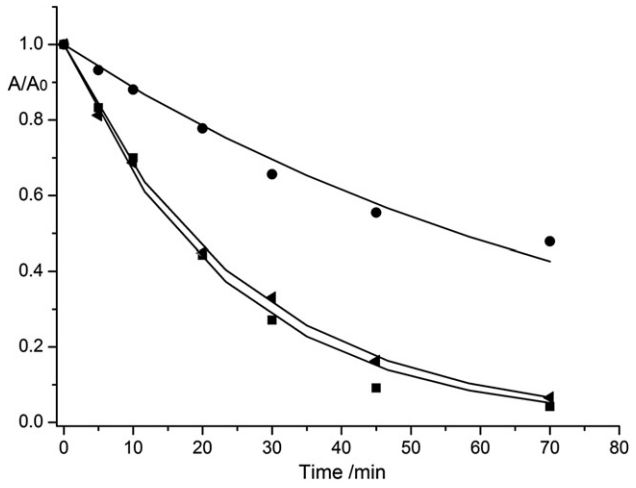

Fig. 6. The photobleaching decay curve of 25 μM LDP (square points and line); in the presence of 1.1 equiv CB[7] (triangle points and line), and in the presence of 50 equiv CB[7] (circle points and line) at pH = 9.6.

experiments of 25 μM LDP aqueous solution in the presence of 1.1 equiv of CB[7] (the mole fractions of LDP, LDP·CB and LDP·CB_2 are calculated as 63%, 33.4% and 3.6% respectively) were also carried out as shown in Fig. 6 and the photobleaching rate in this condition is calculated as $k_{LC1} = 0.039\ min^{-1}$, which is almost the same as LDP ($k_L = 0.042\ min^{-1}$). This result further verifies that, in the [2]pseudorotaxne, CB[7] moves fast between the two moieties instead of staying at either side, and in this dynamic situation, CB[7] could not afford enough protection to keep the chromophore from being decomposed.

4. Conclusions

In summary, a stable [3]pseudorotaxane complex is constructed by simply mixing the linear cyanine dye LDP guest and CB[7] host in aqueous solution, the threading of one LDP molecule into two CB[7] mcrocycles gives rise to a 32 nm bathochromic shift in the absorption and a 13 folds of fluorescent enhancement. It is worthy of noting that the photostability of the cyanine dye is distinctively improved after the encapsulation by CB[7], which may offer a new route to enhance the light-resistance of dyes.

Acknowledgements

This work is financially supported by the NSFC/China (21072058), National Basic Research 973 Program (2011CB808400), and the Foundation for the Author of National Excellent Doctoral Dissertation of PR China (200758).

References

[1] Wang QC, Qu DH, Ren J, Xu LH, Liu MY, Tian H. New benzo[e]indolinium cyanine dyes with two different fluorescence wavelengths. Dyes and Pigments 2003;59:163–72.
[2] Zheng QD, Yao ZG, Chen JQ, Shen YC, Lu ZH. Synthesis and nonlinear optical properties of *p*-(dimethylamino)benzylidene dyes containing different acceptors. Chem Lett 2000;29:1426–7.
[3] Waggoner A. Fluorescent labels for proteomics and genomics. Curr Opin Chem Biol 2006;10:62–6.
[4] Santos PF, Reis LV, Almeida P, Oliveira AS, Ferreira LFV. Singlet oxygen generation ability of squarylium cyanine dyes. J Photochem and Photobiol A Chem 2003;160:159–61.
[5] Chen XQ, Nam SW, Kim GH, Song N, Jeong Y, Shin I, et al. A near-infrared fluorescent sensor for detection of cyanide in aqueous solution and its application for bioimaging. Chem Commun 2010;46:8953–5.
[6] Bin Y, Huang L, Zhao F, Zhang F. Twenty-year overview of the recording materials for three-generation recordable optical discs. Prog Chem 2008;20:1816–26.
[7] Funabiki K, Mase H, Hibino A, Tanaka N, Mizuhata N, Sakuragi Y, et al. Synthesis of a novel heptamethine-cyanine dye for use in near-infrared active dye-sensitized solar cells with porous zinc oxide prepared at low temperature. Energy Environ Sci 2011;4:2186–92.
[8] Kopaindky B, Qiu P, Kaiser W, Sens B, Drexhage KH. Lifetime, photostability, and chemical structure of IR heptamethine cyanine dyes absorbing beyond 1μm. Appl Phys B 1982;29:15–8.
[9] Kawakami M, Suzuki M, Kawai H, Ogawa K, Shishido T. A self-sensitized photoreaction of rhodacyanine dye, MKT 077. Tetra Lett 1998;39:1763–6.
[10] Zhang F, Sautter K, Larsen AM, Findley DA, Davis RC, Samha H, et al. Chemical vapor deposition of three aminosilanes on silicon dioxide: surface characterization, stability, effects of silane concentration, and cyanine dye adsorption. Langmuir 2010;16:14,648–14,654.
[11] Craig MR, Hutchings MG, Claridge TDW, Anderson HL. Rotaxane-encapsulation enhances the stability of an azo dye, in solution and when bonded to cellulose. Angew Chem Int Ed 2001;6:1071–4.
[12] Gadde S, Batchelor EK, Weiss JP, Ling YH, Kaifer AE. Control of H- and J-aggregate formation via host–guest complexation using cucurbituril hosts. J Am Chem Soc 2008;130(50):17,114–17,119.
[13] Mohanty J, Nau WM. Ultrastable rhodamine with cucurbituril. Angew Chem Int Ed 2005;44:3750–4.
[14] Kim J, Jung IS, Kim SY, Lee E, Kang JK, Sakamoto S, et al. New cucurbituril homologues: syntheses, isolation, characterization, and X-ray crystal structures of cucurbit[n]uril (n) 5, 7, and 8. J Am Chem Soc 2000;122:540–1.
[15] Marquet J, Cayon E, Martin X, Casado F, Gallardo I, Moreno M, et al. Topologically controlled coulombic interactions, a new tool in the developing of novel reactivity. photochemical and electrochemical cleavage of phenyl alkyl ethers. J Org Chem 1995;60:3814–25.
[16] Zhang HY, Wang QC, Liu MH, Ma X, Tian H. Switchable V-type [2]pseudorotaxanes. Org Lett 2009;11:3234–7.
[17] Sindelar V, Cejas MA, Raymo FM, Kaifer AE. Tight inclusion complexation of 2,7-dimethyldiazapyrenium in cucurbit[7]uril. New J Chem 2005;29:280–2.
[18] Ko YH, Kim H, Kim Y, Kim K. U-shaped conformation of alkyl chains bound to a synthetic host. Angew Chem Int Ed 2008;47:4106–9.
[19] Curiel D, Hayes EJ, Beer PD. Fluorescent anion complexation agents. ChemInform 2006;37:59–118.
[20] Wagner BD, Stojanovic N, Day AI, Blanch RJ. Host Properties of cucurbit[7]uril: fluorescence enhancement of anilinonaphthalene sulfonates. J Phys Chem B 2003;107:10,741–10,746.
[21] Singh MK, Pal H, Koti ASR, Sapre AV. Photophysical properties and rotational relaxation dynamics of neutral red bound to β-cyclodextrin. J Phys Chem A 2004;108:1465–74.
[22] Choudhury SD, Mohanty J, Upadhyaya HP, Bhasikuttan AC, Pal H. Photophysical studies on the noncovalent interaction of thioflavin T with cucurbit[n]uril macrocycles. J Phys Chem B 2009;113:1891–8.
[23] Bushmann HJ. The selective removal of dye stuffs and heavy metal ions from waste waters of the textile industry. Vom Wasser 1995;84:263–9.
[24] Chen P, Li J, Qian ZG, Zheng DS, Okasaki T, Hayami M. Study on the photooxidation of a near-infrared-absorbing benzothiazolone cyanine dye. Dyes and Pigments 1998;37:213–22.
[25] Kanoy C, Akerman B, Tuite E. Photobleaching of asymmetric cyanine used for fluorescence imaging of single DNA molecules. J Am Chem Soc 2001;123:7985–95.
[26] Tung CH. Fluorescent peptide probes for in vivo diagnostic imaging. Biopolym (Pept Sci) 2004;76:391–403.
[27] Yang SJ, Meng FS, Tian H, Yao SD. Study on the photodegradation mechanism of cyanine dyes and merocyanine dyes solution. Photogr Sci Photochem 2001;19:169–76.